

 University of Southampton	<b>MERIS ESL</b>	Doc: Name: ATBD: Chlorophyll Index Issue : 1      Revision: 2 Date : 16.09.2005
--	----------------------	--

# **ALGORITHM THEORETICAL BASIS DOCUMENT**

## **ATBD 2.22**

### **CHLOROPHYLL INDEX**

**Version-2.2**

**Paul J. Curran<sup>1</sup> and Jadunandan Dash<sup>2</sup>**

**<sup>1</sup>Vice-Chancellor,  
Bournemouth University  
Poole, Dorset, United Kingdom  
<sup>2</sup>School of Geography,  
University of Southampton  
Southampton, United Kingdom**

# Content

<b>1. INTRODUCTION</b> .....	<b>1</b>
<b>2. ALGORITHM OVERVIEW</b> .....	<b>1</b>
2.1. OBJECTIVE .....	1
2.2. INSTRUMENT CHARACTERISTICS .....	3
2.3. RETRIEVAL STRATEGY .....	3
<b>3. ALGORITHM DESCRIPTION</b> .....	<b>4</b>
3.1. THEORETICAL DESCRIPTION .....	4
3.1.1 <i>Physics of the problem</i> .....	4
3.1.2 <i>Mathematical description of the algorithm</i> .....	8
3.1.2.1. Indirect MTCI evaluation .....	12
3.1.2.2. Conclusion .....	14
3.1.3 <i>Effect of different variables</i> .....	15
3.1.3.1. Atmospheric correction .....	15
3.1.3.2. Spatial resolution .....	23
3.1.3.3. Soil brightness .....	24
3.1.3.4. View angle .....	24
3.2. PRACTICAL CONSIDERATIONS .....	25
3.2.1 <i>Calibration and validation</i> .....	25
3.2.2 <i>Quality control and diagnostics</i> .....	28
3.2.3 <i>Output</i> .....	29
<b>4. ASSUMPTIONS AND LIMITATIONS</b> .....	<b>29</b>
4.1. ASSUMPTIONS .....	29
4.2. LIMITATIONS .....	30
<b>5. REFERENCES</b> .....	<b>31</b>

## List of Figures

Figure 1. MERIS level 2 processing for Land.

Figure 2. (a) Illustrative vegetation reflectance spectra at four chlorophyll contents (model output) overlain with the position of MERIS bands 8, 9 and 10. (b) Relation between the MERIS terrestrial chlorophyll index (MTCI) and red edge position (REP) for four chlorophyll contents.

Figure 3. Reflectance of sediment laden water in MERIS red and NIR wavebands for two points (point\_1 and Point\_2).

Figure 4. Description of Algorithm used for MTCI calculation.

Figure 5. (a) Reflectance spectra for MERIS data at the standard band settings, simulated using the LIBSAIL model for a wide range of chlorophyll contents; (b) relation between chlorophyll content and MTCI for the same range of chlorophyll contents and (c) relation between REP and chlorophyll content for the same range of chlorophyll contents.

Figure 6. MERIS images of southern England (a) NDVI image (b) REP image (c) MTCI image.

Figure 7. Effect of atmospheric correction on the estimation of MTCI. A) MTCI image generated using atmospherically-corrected L1 data. B) MTCI image generated using normalised surface reflectance from L2 data (without masking the ocean). C) MTCI image generated using normalised surface reflectance from L2 data (after masking the ocean).

Figure 8. Cumulative percentage of MTCI maximum for 8 test sites in Vietnam (MTCI estimated from L2 data).

Figure 9. Cumulative percentage of MTCI maximum for 8 test sites in Vietnam (MTCI estimated from L1 data).

Figure 10. Cumulative percentage of MTCI maximum for 3 test sites in the UK (MTCI estimated from L2 data).

Figure 11. Cumulative percentage of MTCI maximum for 3 test sites in the UK (MTCI estimated from L1 data).

Figure 12. Cumulative percentage of MTCI maximum for 5 test sites representing four different vegetation in West Africa (MTCI estimated from L2 data).

Figure 13. Cumulative percentage of MTCI maximum for 5 test sites, representing 4 different vegetation in West Africa (MTCI estimated from L1 data).

Figure 14. Vegetation types superimposed on an MTCI for West Africa.

Figure 15. SD of MTCI for different spatial resolutions

Figure 16. Cumulative percentage of MTCI maximum for different spatial resolutions.

Figure 17. Relationship between chlorophyll content and SR (a), NDVI (b), REP estimated by maximum of first derivative (c), REP estimated by linear interpolation (d), REP estimated by Lagrangian interpolation (e) and MTCI (f) for spinach.

## **List of Tables**

Table 1. Characteristic spectral features of foliar biochemicals (adapted from Curran 1980).

Table 2. Correlation coefficient between the reflectance indices and chlorophyll content for spinach sample.

Table 3. Comparison of cumulative % of MTCI ranges for MTCI estimated from L2 data (L2) and atmospherically corrected L1 data (AC) for Vietnam

Table 4 Comparison of cumulative percentage of MTCI ranges for MTCI estimated from L2 data (L2) and atmospherically corrected L1 data (AC) for UK

Table 5 Comparison of cumulative percentage of MTCI ranges for MTCI estimated directly from L2 data (L2) and atmospherically corrected L1 data (AC) for West Africa.

## **1. Introduction**

This Algorithmic Theoretical Basis Document (ATBD) describes an algorithm used to estimate chlorophyll content over land from Level-1b MERIS products. The algorithm called the MERIS Terrestrial Chlorophyll Index (MTCI) is a unique chlorophyll index for MERIS data.

This document identifies the source of input data; outlines the physical principles and mathematical background; justifies this algorithm and then explores its limitations and assumptions.

## **2. Algorithm Overview**

The algorithm described here is called the MERIS Terrestrial Chlorophyll Index (MTCI); it is suitable for monitoring vegetation condition from MERIS data and so is a partner to the MERIS Global Vegetation Index (MGVI) (figure 1).

### **2.1. Objective**

Remotely sensed data recorded in narrow visible/near visible wavebands can be used to estimate foliar biochemical content at local to regional scales (Curran 1989, Curran et al. 1997). This information can, in turn, be used to quantify, understand and manage vegetated environments (Curran 2001, Johnson 1999, Lamb et al. 2002). Chlorophyll is one of the more important foliar biochemicals and the content within a vegetation canopy is related positively to both the productivity of that vegetation and the depth and width of the chlorophyll absorption feature in the reflectance spectra. The long wavelength (red) edge of this absorption feature moves to even longer wavelengths with an increase in chlorophyll content (Curran et al. 1990, Filella and Peñuelas 1994, Munden et al. 1994) and the red edge position (REP) can be defined as the point

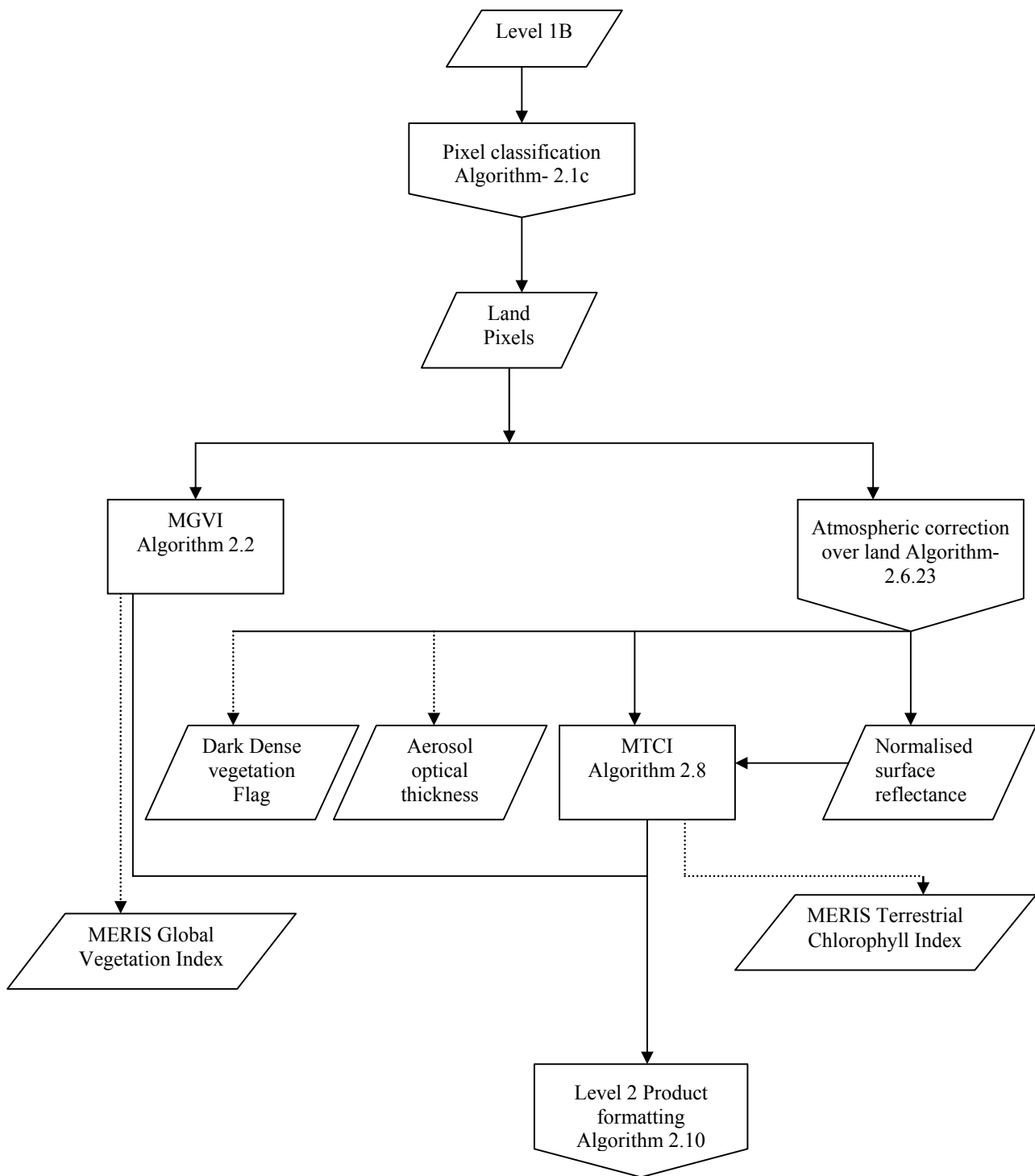


Figure 1. MERIS level 2 processing for Land.

of maximum change in reflectance along this edge (Horler et al. 1983). However, there are two problems with the use of REP to estimate foliar chlorophyll content from a spaceborne sensor.

First, the methods used to estimate REP have been designed for use on continuous spectra without thought for standardisation or automation (Dawson and Curran 1998). Second, REP is not an accurate indicator of chlorophyll content at high chlorophyll contents because of the asymptotic relationship between REP and chlorophyll content (Jago et al. 1999, Munden et al. 1994).

The MERIS Terrestrial Chlorophyll Index is designed to exploit spectral reflectance, in the red and near-infrared wavelengths, acquired by MERIS and provide reliable quantitative information on terrestrial chlorophyll content.

## **2.2. Instrument characteristics**

The MERIS instrument has been well described in a number of publications ( Rast et al. 1999; Curran and Steele 2004). For the purpose of this document, it is sufficient to recall that MERIS, one of the payloads on Envisat, is radiometrically the most accurate imaging spectrometer in space (Curran and Steele 2004). It has 15 programmable (2.5 nm-20 nm wide) wavebands in the 390 nm - 1040 nm region and spatial resolutions of 300 m and 1200 m. Because of its fine spectral resolution, moderate spatial resolution and three day repeat cycle, MERIS is a potentially valuable sensor for the measurement and monitoring of terrestrial environments at regional to global scales (Verstraete et al. 1999). In the standard band setting, it has 5 discontinuous wavebands in red (R) and near infrared (NIR) wavelengths with band centres at 665 nm, 681.25 nm, 708.75 nm, 753.75 nm and 760.625 nm.

## **2.3. Retrieval strategy**

Two techniques have been used to estimate the REP on discontinuous (simulated) MERIS spectra: Lagrangian interpolation (Dawson 2000) and linear interpolation (Clevers et al. 2002). As indicated earlier, each of these techniques produces a different value of REP and REP values are relatively insensitive to chlorophyll content at high values of chlorophyll content. Therefore, a surrogate REP index, the MTCI, for use with spectral data recorded at the standard band settings of the MERIS is proposed.

Following criteria for the design of MTCI were considered:

1. Sensitive to a wide range of chlorophyll contents
2. Estimation of the MTCI value requires minimal computational costs.
3. Estimation of chlorophyll content with MTCI is independent of soil and atmospheric condition, spatial resolution and illumination and observation geometry.

### **3. Algorithm description**

#### **3.1. Theoretical description**

##### **3.1.1 Physics of the problem**

The spectral reflectance of vegetation contains absorption features that are result of electron transitions and vibrational stretching of organic and inorganic bonds. The main chemical constituent of leaves include chlorophyll, water, nitrogen and carbon containing compounds, comprising primarily protein, lignin and cellulose. Out of these chlorophyll is associated with the process of photosynthesis and together with water, temperature, nutrient availability, CO<sub>2</sub> and sunlight; determines the rate of primary productivity. Therefore, chlorophyll is an important driver for the whole ecosystem (Munden et al. 1994).

When incoming radiation interacts with vegetation, some part of it is reflected, some absorbed and rest is transmitted. A typical reflectance spectrum of a vegetation canopy can be subdivided into 3 parts, visible (400- 700 nm), near-infrared(NIR) (701 – 1300 nm) and middle-infrared (1301- 2500 nm).

Chlorophyll is the major absorber of radiation in the visible region. Chlorophylls are of two types, chlorophyll-a and chlorophyll-b; chlorophyll-a content is usually two to three times that of chlorophyll-b and dominates absorption in 600-700 nm wavelengths (Lichtenthaler 1987). Other leaf pigments also have an important effect on the visible spectrum. For example, the yellow to orange-red pigment, carotene, has a strong absorption in the 350 - 500 nm range and is responsible for the colour of some flowers and fruits as well as leaves without chlorophyll. The red and blue pigment, xanthophyll, has strong absorption in the 350-500 nm range and is responsible for the leaf colour in autumn.

In the near-infrared spectral domain (701-1300 nm), leaf structure explains the optical properties. Near-infrared spectral region can be divided into two major spectral sub-regions: first, between 701 and 1100 nm, where reflectance is high, except in two minor water-related absorption bands (960 and 1100 nm) and second, between 1100 and 1300 nm, which corresponds to the transition between high near-infrared reflectance and water-related absorption bands of the middle infrared. The intensity of NIR reflectance is commonly greater than from most inorganic materials, so vegetation appears bright in NIR wavelengths.

The middle-infrared region contains information about the absorption of radiation by water, cellulose and lignin etc. Other biochemicals, which contribute to absorption in middle infra-red wavelengths, are starches, sugars, lipids and minerals. Curran (1989) presented a list of

forty-four absorption features in the visible and near-infrared wavelengths which were related to foliar biochemical constituents.

The relations between multispectral reflectance and vegetation amount for six wavebands (Curran 1980) are summarised in table 1.

Waveband	Waveband width (nm)	Characteristics	Relation to vegetation amount
<b>Ultraviolet/blue</b>	350-500	Strong chlorophyll and carotene absorption	Strong negative
<b>Green</b>	500-600	Reduced level of pigment absorption	Weak positive
<b>Red</b>	600-700	Strong chlorophyll absorption	Strong negative
<b>Red edge</b>	700-740	Transition between strong absorption and strong reflectance	Weak negative
<b>Near-infrared</b>	740-1300	High vegetation reflectance	Strong positive
<b>Middle-infrared</b>	1300-2500	Water, cellulose and lignin absorption	Not specific

Table 1. Characteristic spectral features of foliar biochemicals (adapted from Curran 1980).

The red edge is a region within the red-NIR transition zone of a vegetation reflectance spectrum and marks the boundary between absorption due to chlorophyll in the red region and scattering due to leaf internal structure in the NIR region (Horler et al. 1983). The red edge position (REP) can be defined as the maximum of the first derivative of the reflectance spectra of a leaf (Horler et al. 1983; Curran et al. 1990). According to the Beer-Lambert law a negative exponential correlation exists between chemical concentration and absorption. Therefore an increase in chlorophyll concentration increases absorption. This in turn will cause both broadening and deepening of the absorption feature (Filella and Peñuelas 1994; Curran et al.

1995) and a movement of the REP to longer wavelengths. This change in the REP can be used to estimate the amount of chlorophyll both in a leaf and over a canopy (Munden et al. 1994; Pinar and Curran 1994; Railyan and Korobov 1993).

Mathematically, REP is the maximum of the first derivative spectrum in the red edge region. The derivative spectrum can be estimated by

$$D_{\lambda(i)} = \frac{R_{\lambda(i)} - R_{\lambda(i-1)}}{\Delta\lambda} \quad (1)$$

Where,  $R_{\lambda(i)}$  and  $R_{\lambda(i-1)}$  are reflectances at wavelength  $i$  and  $(i-1)$  respectively. The REP estimated using the maximum of first derivative method is accurate if the sensor has fine spectral resolution and also this process eliminates/reduces the source of variability, for example, background reflectance from the reflectance spectra (Horler et al. 1983; Demetriades-Shah 1990). However, an accurate estimation of REP using maximum of first derivative method requires both spectral continuity and fine spectral resolution of the reflectance spectra (Dawson and Curran 1998). To overcome this dependency on spectral sampling intervals researchers suggested different techniques for REP estimation. Most commonly used techniques include (i) higher order curve fitting techniques (Demetriades-Shah 1990); (ii) an inverted Gaussian technique (Bonham-Carter 1988; Miller et al. 1990); (iii) a linear interpolation technique (Guyot et al. 1988, Danson and Plummer 1995) and (iv) a Lagrangian interpolation technique (Dawson and Curran 1998).

Undoubtedly REP techniques will be applied to MERIS data for the estimation of chlorophyll content. However, (i) there remains no generally accepted technique for estimation of REP, (ii) each technique produces a different value of REP from the same set of data and (iii) neither of the techniques listed above offer the automated, one-step procedure that would be required for the processing of large volume data at, for example, a ground receiving station.

Therefore, a new index for estimating chlorophyll content from MERIS data has been designed as a surrogate for REP.

### 3.1.2 Mathematical description of the algorithm

The proposed algorithm to compute MTCI can be explained with the following example (figure 1). *Illustrative* vegetation reflectance spectra (model output) are given in figure 2a, with chlorophyll content increasing from spectrum 1 to spectrum 4. An increase in absorption due to an increase in chlorophyll content is seen in the wavelength range 650 - 700 nm. Reflectance increases sharply as we move from MERIS band 8 to band 10 for a particular chlorophyll content (figure 2a).

However, comparison of the four illustrative reflectance spectra reveals two important features:

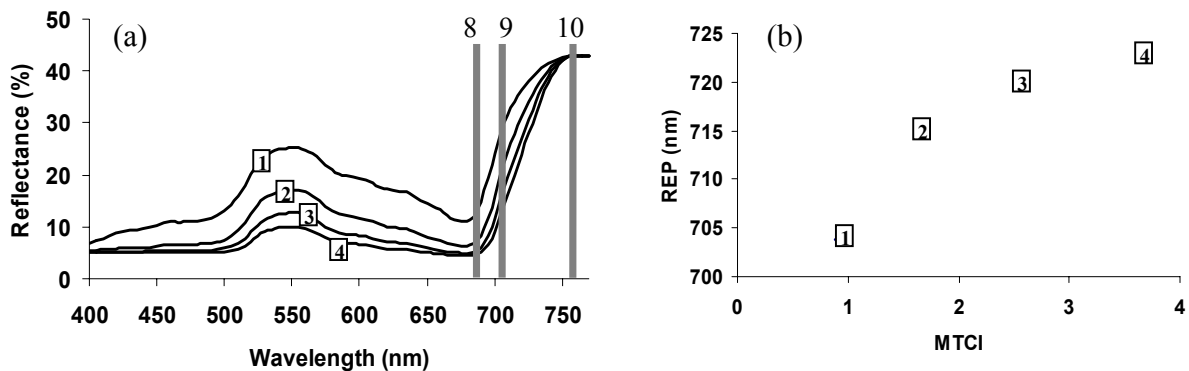


Figure 2 (a) Illustrative vegetation reflectance spectra at four chlorophyll contents (model output) overlain with the position of MERIS bands 8, 9 and 10. (b) Relation between the MERIS terrestrial chlorophyll index (MTCI) and red edge position (REP) for four chlorophyll contents.

(i) with an increase in chlorophyll content the difference in reflectance between band 8 and band 9 decreases gradually and (ii) with an increase in chlorophyll content the difference in reflectance between band 9 and band 10 increases gradually. The MERIS Terrestrial Chlorophyll Index

(MTCI) is a ratio of the difference in reflectance between band 10 and band 9 and the difference in reflectance between band 9 and band 8 of the MERIS standard band setting.

$$MTCI = \frac{R_{Band10} - R_{Band9}}{R_{Band9} - R_{Band8}} = \frac{R_{753.75} - R_{708.75}}{R_{708.75} - R_{681.25}} \quad (2)$$

Where  $R_{753.75}$ ,  $R_{708.75}$ ,  $R_{681.25}$  are reflectance in the centre wavelengths of the MERIS standard band setting.

Figure 2b illustrates the relation between MTCI and REP for the four illustrative spectra in figure 1a. The REP calculated using linear interpolation is illustrated here because of its simplicity, however, REP calculated using Lagrangian interpolation provided similar, albeit linearly offset, results. It can be seen that there is little change in REP but a large change in MTCI between high chlorophyll contents. This implies that MTCI is more sensitive to change in chlorophyll content at high chlorophyll contents than is REP.

MTCI requires atmospherically corrected reflectance, in other word, top-of-canopy reflectance. However, it is not possible within the MERIS processor to perform a proper atmospheric correction. The best available data for MTCI calculation was Rayleigh corrected surface reflectance in individual bands. Further description about the atmospheric correction above land can be found in the MERIS user's handbook (ESA, 2005).

Three possible features: sediment laden water, barren and low cloud cover could be a source of ambiguity in the MTCI estimation. Therefore, prior to the calculation of MTCI pixels covering these features should be removed.

For sediment laden water, reflectance in MERIS band 8, 9 and 10 varies with change in sediment concentration (figure 3). In most cases MTCI estimated for pixels covering sediment laden water varies with sediment concentration and fall within the MTCI range for vegetation. Therefore,

pixels covering sediment laden water should be removed from the scene to avoid confusion with vegetation.

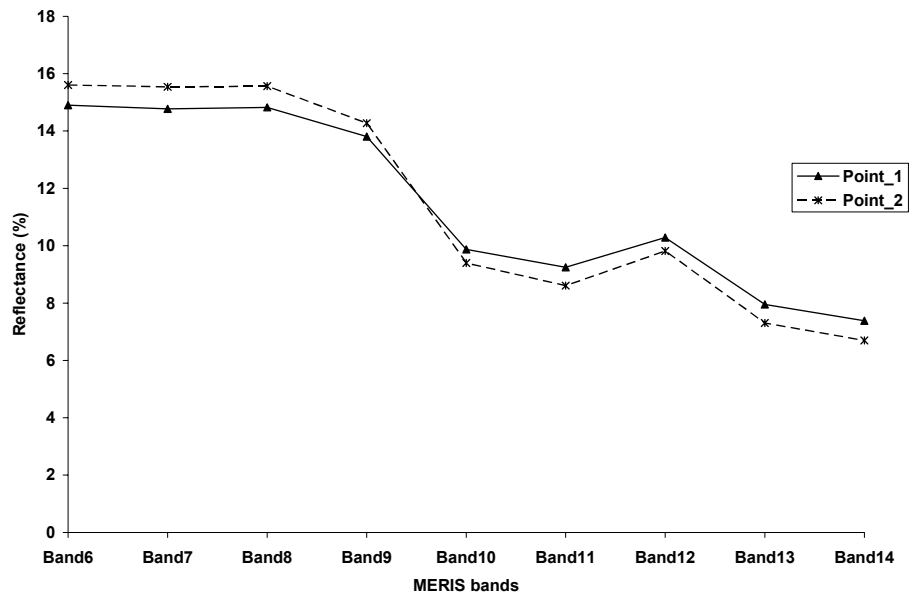


Figure 3. Reflectance of sediment laden water in MERIS red and NIR wavebands for two points (point\_1 and Point\_2).

Unlike the vegetated pixel these pixels have very low NIR reflectance; therefore it was decided to remove pixels with reflectance less than 0.1 NIR (MERIS band 13) in order to keep only land pixels.

Next task was to remove the non vegetated land pixels, i.e. pixels which are barren. Absorption in the red region was used to distinguish between the vegetated and barren pixels. It was assumed that pixel having high red reflectance (greater than 0.3) are non barren. Therefore pixels having reflectance at MERIS band 8 greater than 0.3 were removed.

Pixels with low cloud cover are not removed during atmospheric correction. The reflectance in these pixels is a mixture of reflectance from ground and top of the cloud. Therefore, MTCI estimated for these pixels are not representative of the ground vegetation condition. These pixels should be removed to avoid confusion. It was assumed that, for these pixels there will be very less difference in red and NIR reflectance. Therefore, pixels where difference in reflectances between band 13 and band 8 was less than 0.05 were flagged.

**For each pixel (j,f) such that (INVALID\_F(j,f) == FALSE) AND (LANDCONS\_F(j,f) = TRUE)**

*Exception processing*

**WHEN** (  $\rho_{top}(mtci\_red\_band,j,f) \leq 0$ ) **OR**  
(  $\rho_{top}(mtci\_nir1\_band,j,f) \geq \rho_{red\_max}$  **OR**  
 $\rho_{top}(mtci\_nir2\_band,j,f) \geq \rho_{nir2\_min}$  **OR**  
 $|\rho_{top}(mtci\_nir1\_band,j,f) - \rho_{top}(mtci\_nir2\_band,j,f)| < \rho_{diff\_min}$ :  
**OR**INP2\_F(j,f)=TRUE  
MTCI(j,f)= BAD\_VALUE)

*End of exception processing*

$$MTCI(j, f) = \frac{\rho_{top}(mtci\_nir2\_band, j, f) - \rho_{top}(mtci\_nir1\_band, j, f)}{\rho_{top}(mtci\_nir1\_band, j, f) - \rho_{top}(mtci\_red\_band, j, f)}$$

**If**(MTCI(j,f)<MTCI\_RANGE(0))**OR**(MTCI(j,f)>MTCI\_RANGE(1)) **THEN**  
**OR**INP2\_F(j,f)=TRUE  
MTCI(j,f)= BAD\_VALUE  
**ENDIF**

Figure 4. Description of *Algorithm* used for MTCI calculation.

### 3.1.2.1. Indirect MTCI evaluation

Data from model, laboratory and field measurements, real MERIS data were used for indirect evaluation the MTCI.

#### *Model data*

Vegetation reflectance obtained from LIBSAIL (combination of LIBERTY (Leaf Incorporating Biochemistry Exhibiting Reflectance and Transmittance Yield (Dawson et al. 1998)) and SAIL (Scattering by Arbitrary Inclined Leaves (Verhoef 1984)) spectra for simulated MERIS band positions over a wide range of chlorophyll contents ( $10 \text{ mg m}^{-2}$  to  $400 \text{ mg m}^{-2}$ ) are shown in figure 5a. Estimated MTCI and REP for each spectrum are given in figures 5b and 5c respectively.

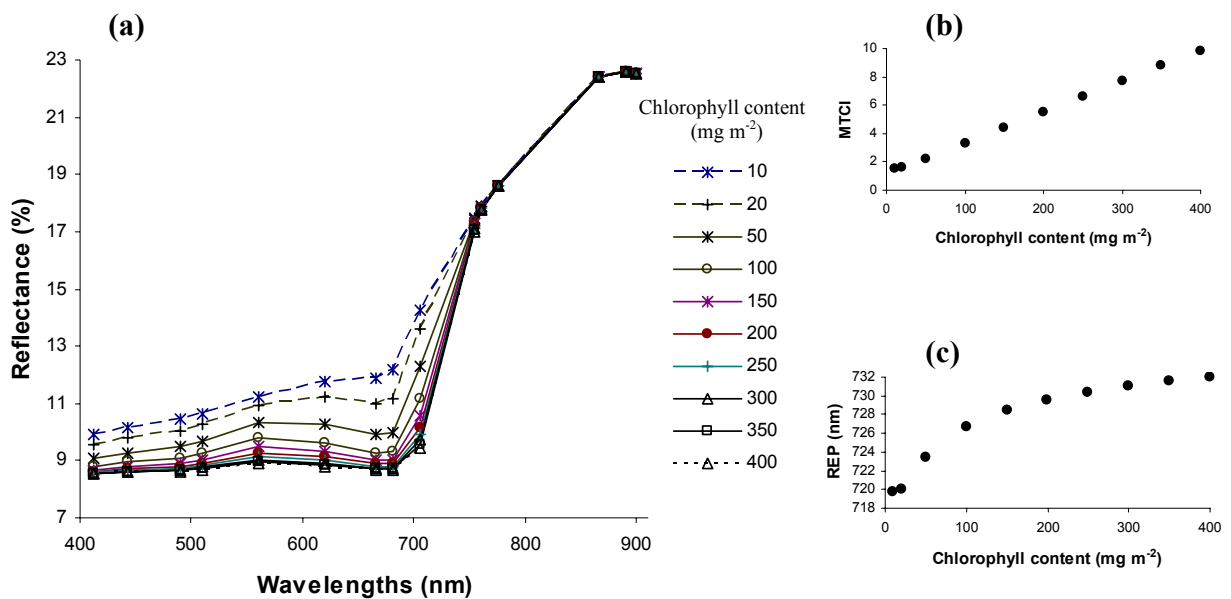


Figure 5 (a) Reflectance spectra for MERIS data at the standard band settings, simulated using the LIBSAIL model for a wide range of chlorophyll contents; (b) relation between chlorophyll content and MTCI for the same range of chlorophyll contents and (c) relation between REP and chlorophyll content for the same range of chlorophyll contents.

The asymptotic relationship between REP and chlorophyll content (figure 5c) suggested insensitivity to high chlorophyll contents; however, the near-linear relationship between MTCI and chlorophyll content (figure 5b), suggested sensitivity to high chlorophyll contents.

#### *Field data*

Canopy reflectance spectra and canopy chlorophyll content data had been collected for monospecific canopies formed from Douglas-fir (*Pseudotsuga menziesii*) and bigleaf maple (*Acer macrophyllum*) seedlings as a part of NASA's 1992-1993 ACCP (Accelerated Canopy Chemistry Program) (Yoder and Johnson 1999).

For Douglas-fir the coefficients of determination were 0.64 and 0.62 between chlorophyll content and first MTCI and second REP. Similarly, for maple the coefficients of determination ( $r^2$ ) were 0.72 and 0.62 between chlorophyll content and first MTCI and second REP. In both the cases, the regression line between MTCI and chlorophyll content had a slightly steeper slope than the regression line between REP and chlorophyll content. This suggested that MTCI was more sensitive than REP to chlorophyll content.

#### *MERIS data*

A subset of a MERIS image acquired on 19<sup>th</sup> October 2002 was extracted for the New Forest, Hampshire, UK. The area comprises coniferous and deciduous woodland along with heath, meadows, agricultural land, urban areas and water.

The NDVI image (figure 6a) is included for reference. This delineated three broad zones (i) vegetated with high NDVI (and assumed high chlorophyll content) in woodland areas near the image centre, (ii) vegetated with intermediate NDVI (and assumed lower chlorophyll content) in heath, meadows and agricultural land towards for example, the western edge of the image and

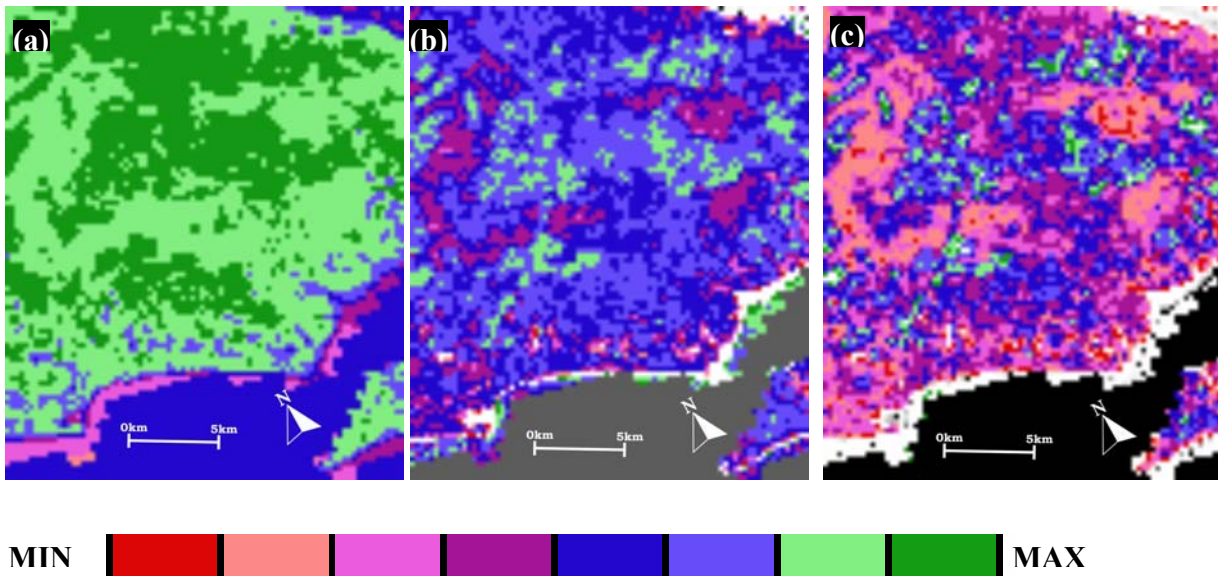


Figure 6 MERIS images of southern England (a) NDVI image (b) REP image (c) MTCI image.

(iii) non-vegetated with, for example, low or negative NDVI values in urban and coastal areas. The REP image (figure 6b) identified some variation within these broad NDVI zones; however, the MTCI image figure 6c) identified greater variation within the broad NDVI zones and this level of variation did not decline with increasing NDVI. This suggested that MTCI was likely to be more sensitive than REP to high values of NDVI and thereby chlorophyll content.

### 3.1.2.2. Conclusion

Preliminary evaluation of MTCI revealed four characteristics that are relevant here:

1. There was only one MTCI value for each pixel (MTCI is an absolute value derived using a specific method, unlike the REP which is a method-specific estimate of an actual value).
2. Calculation of the MTCI could be automated readily, as it involved one step and no manual intervention.

3. Should it be necessary, REP can be estimated from MTCI, as a strong relationship exists between REP and MTCI.
4. MTCI was more sensitive than REP to high chlorophyll contents.

### **3.1.3 Effect of different variables**

#### **3.1.3.1. Atmospheric correction**

Atmospherically corrected L1 data were used for the preliminary evaluation of MTCI. However, when estimating MTCI for standard L2 data the best available input data were normalised surface reflectance, which were not atmospherically corrected. The purpose of this study was to examine the effect of atmospheric correction on the MTCI and determine the minimum and maximum range of the MTCI which can then be scaled into 1 to 255 DN (one byte). A MERIS dataset covering three areas was used: Vietnam, United Kingdom and West Africa.

#### **Processing**

For L1 data atmospheric correction was performed using the Simplified Method for Atmospheric Correction (SMAC) to obtain Top-of-Canopy (TOC) reflectance and MTCI was estimated from these TOC reflectances. For L2 data, MTCI was estimated directly from normalised surface reflectances. Three test sites for UK, eight test sites for Vietnam and five test sites for West Africa were selected to represent different type of vegetation. Cumulative percentages of MTCI in the range 1 to 4.2 were estimated for all test sites.

#### **Observation**

The following four points were observed.

1. Effect of atmospheric correction:

Atmospheric correction had very little effect on the MTCI value estimated at any of the sixteen test sites (e.g. for site-2 in Vietnam most of the MTCI values were distributed between 2 and 3.2

irrespective of data used (table 2)). However use of normalised surface reflectance may produce, in some cases, higher MTCI values (e.g. for site 2 in UK more than 2% MTCI values were greater than 4 (table 2)).

## 2. Effect over ocean

Some of the ocean pixels had positive MTCI values, when MTCI was estimated using normalised surface reflectance from L2 data. Possible reasons may be the reflectance properties of suspended sediments or atmospheric effects over ocean; however, the actual reason is still under investigation. This effect can be removed easily by masking ocean pixels during the estimation of MTCI (figure 7). By way of illustration, figure 7a is an MTCI image derived from atmospherically corrected L1 data and there are no positive MTCI values over ocean; figure 7b is an MTCI image derived from L2 data and many of the ocean pixels have positive MTCI values.

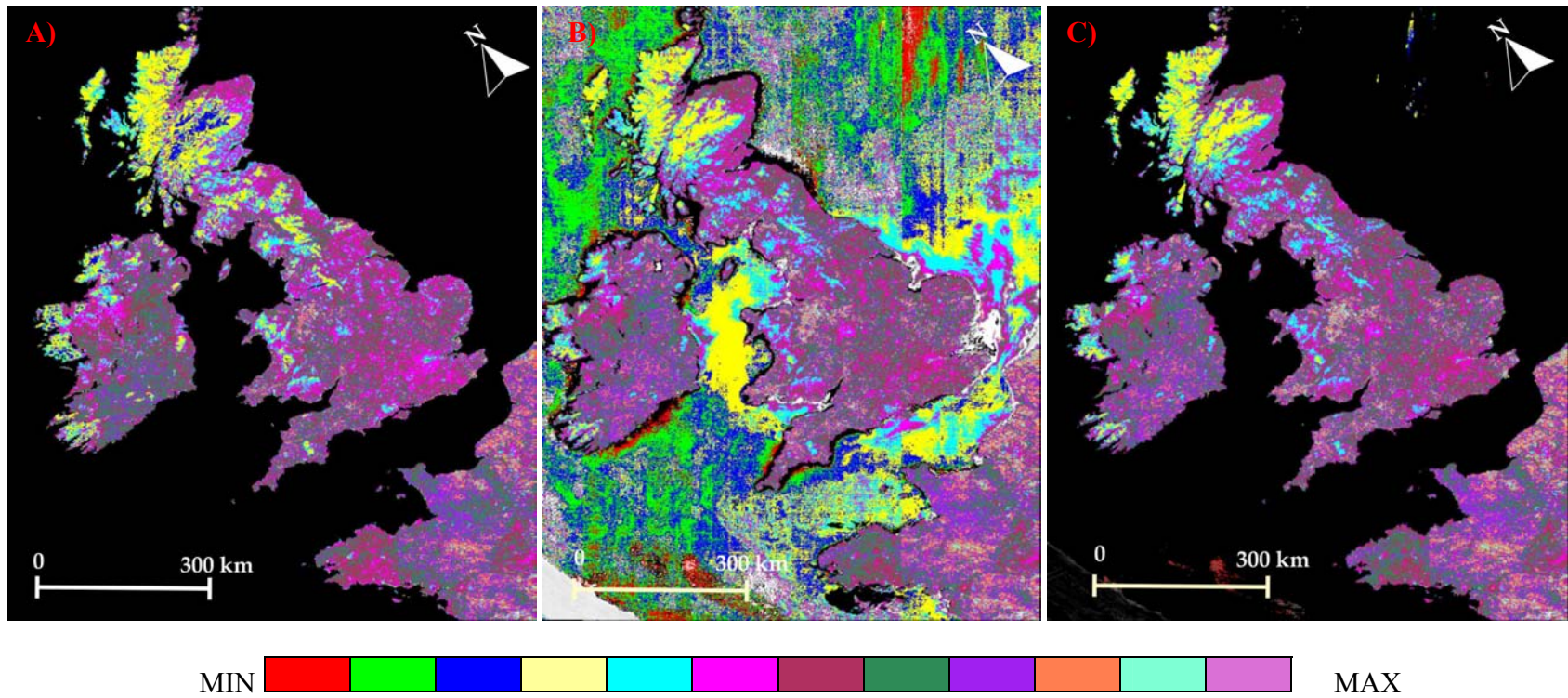


Figure 7: Effect of atmospheric correction on the estimation of MTCI. A) MTCI image generated using atmospherically-corrected L1 data. B) MTCI image generated using normalised surface reflectance from L2 data (without masking the ocean). C) MTCI image generated using normalised surface reflectance from L2 data (after masking the ocean).

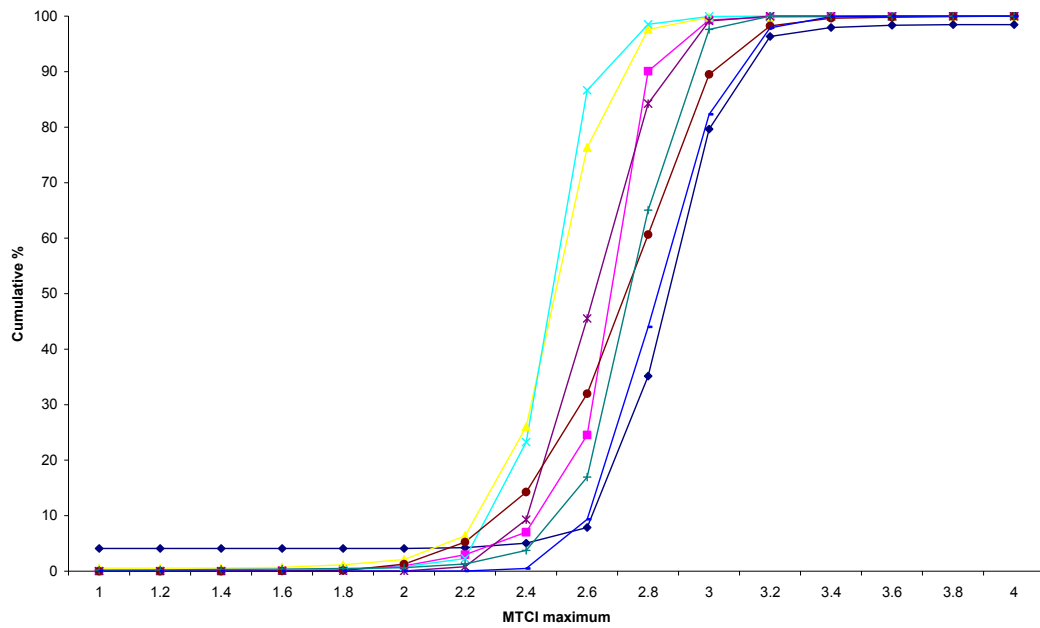


Figure 8 Cumulative percentage of MTCI maximum for 8 test sites in Vietnam (MTCI estimated from L2 data).

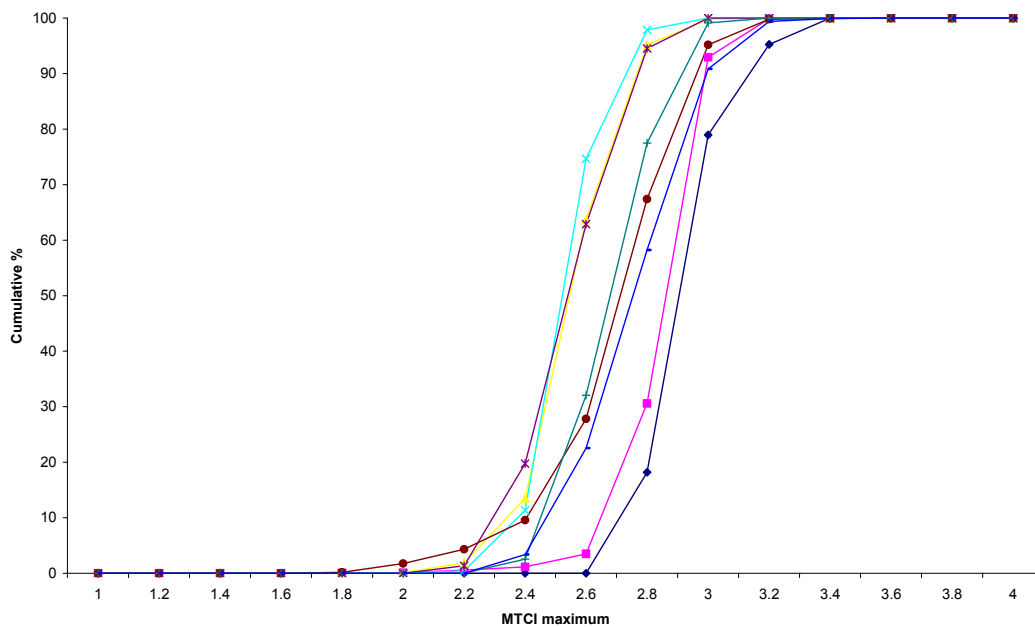


Figure 9 Cumulative percentage of MTCI maximum for 8 test sites in Vietnam (MTCI estimated from L1 data).

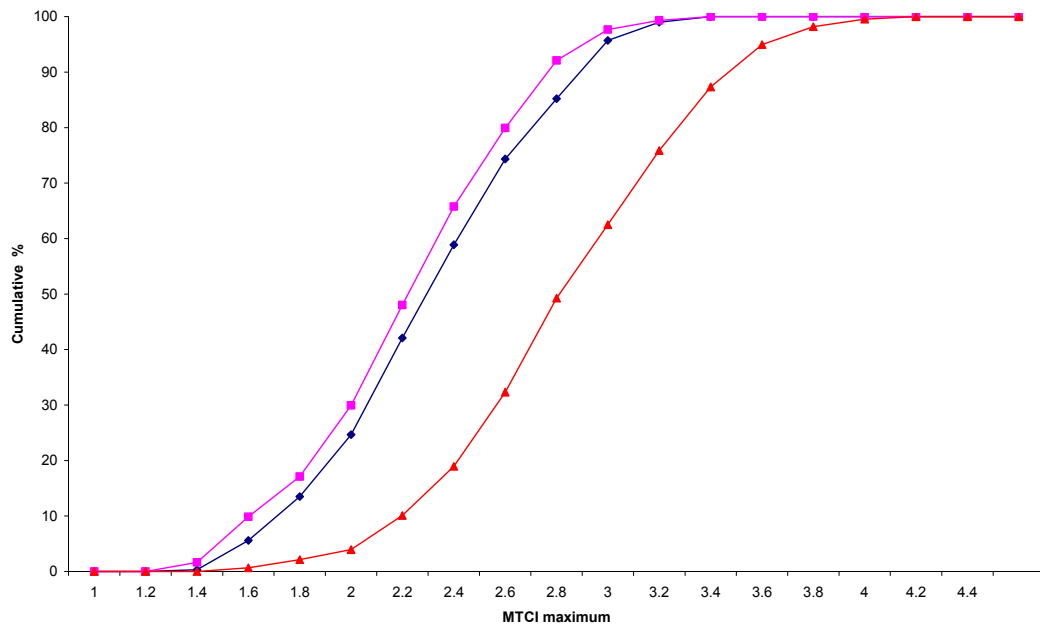


Figure 10 Cumulative percentage of MTCI maximum for 3 test sites in the UK (MTCI estimated from L2 data).

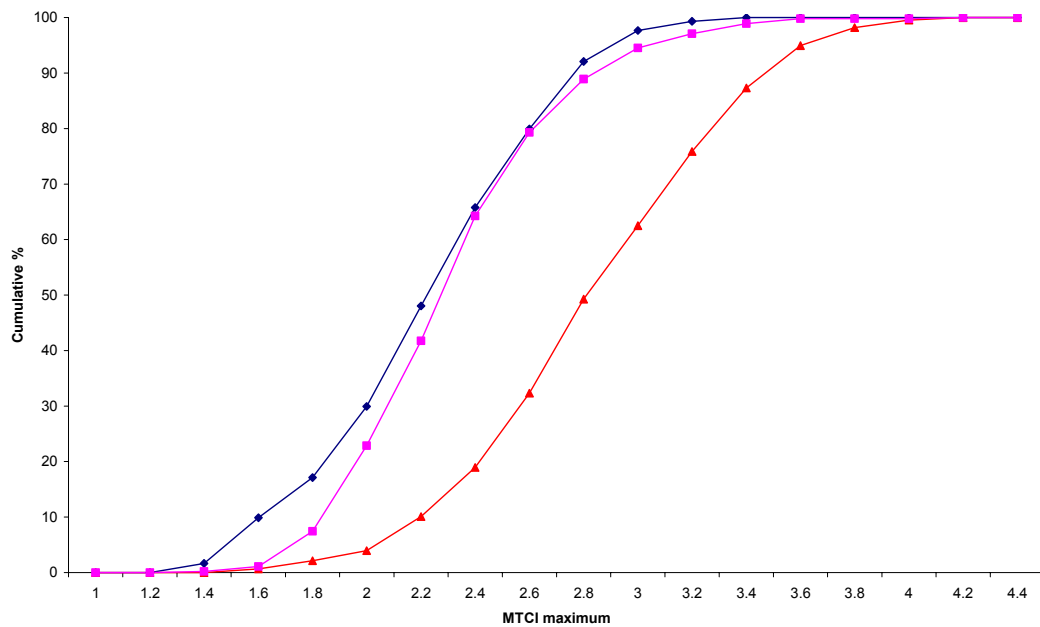


Figure 11 Cumulative percentage of MTCI maximum for 3 test sites in the UK (MTCI estimated from L1 data).

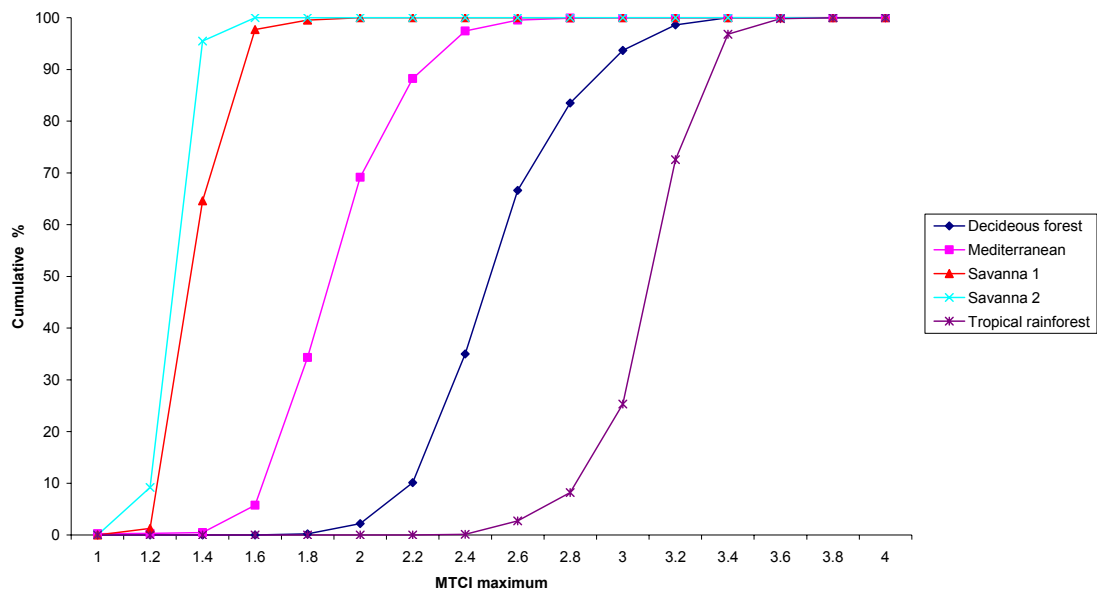


Figure 12 Cumulative percentage of MTCI maximum for 5 test sites representing four different vegetation in West Africa (MTCI estimated from L2 data).

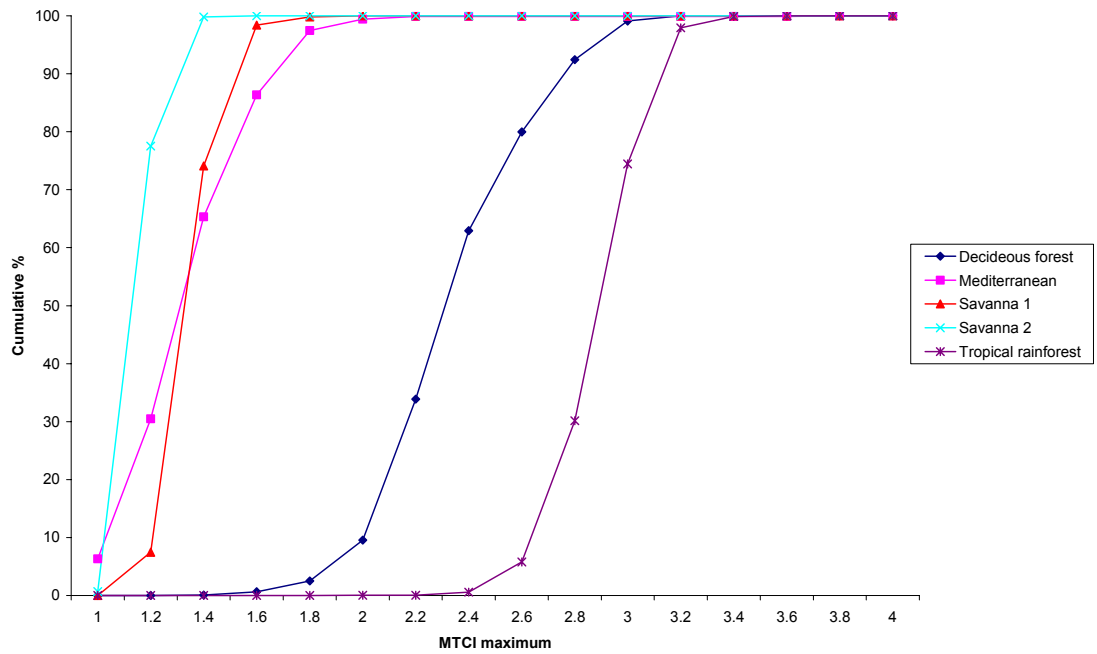


Figure 13 Cumulative percentage of MTCI maximum for 5 test sites, representing 4 different vegetation in West Africa (MTCI estimated from L1 data).

Figure 7c is an MTCI image derived from L2 data with an ocean mask and is very similar to figure 7a, suggesting that atmospheric correction has little or no effect on the estimation of MTCI. Therefore, the effect of the ocean can be removed by masking out these pixels prior to estimation of MTCI over land.

### 3. Distinguishing between vegetation and non-vegetation:

As would be anticipated from the design of the index all vegetation pixels had MTCI values greater than 1 and pixels representing all other land cover type had MTCI values less than 1. In all 16 cases (figures 8 to 13) MTCI maximum were greater than 1 for vegetation pixels. Therefore, to incorporate other land cover types the minimum MTCI value was set to 0.

### 4. Distinguishing between vegetation types

MTCI maximum were different for different type of vegetation. For the West Africa study area five test sites were chosen representing 4 different type of vegetation i.e., tropical rain forest, deciduous forest, savanna and Mediterranean vegetation. Cumulative percentages of MTCI maximum (figures 12 and 13) indicated that the MTCI maximum varied with vegetation type, as each had a different range of chlorophyll content. For example, savannas with relatively low levels of chlorophyll content had MTCI values distributed between 1.2 and 1.5; for tropical forest with relatively high chlorophyll levels of content had MTCI values distributed between 2.4 and 3.6 and the other two vegetation types (i.e. deciduous forest and Mediterranean) had chlorophyll content levels that were intermediate between savannas and tropical forest and as a result had intermediate MTCI values. Figure 14 shows the potential for using an MTCI image as a nominal map of vegetation type.

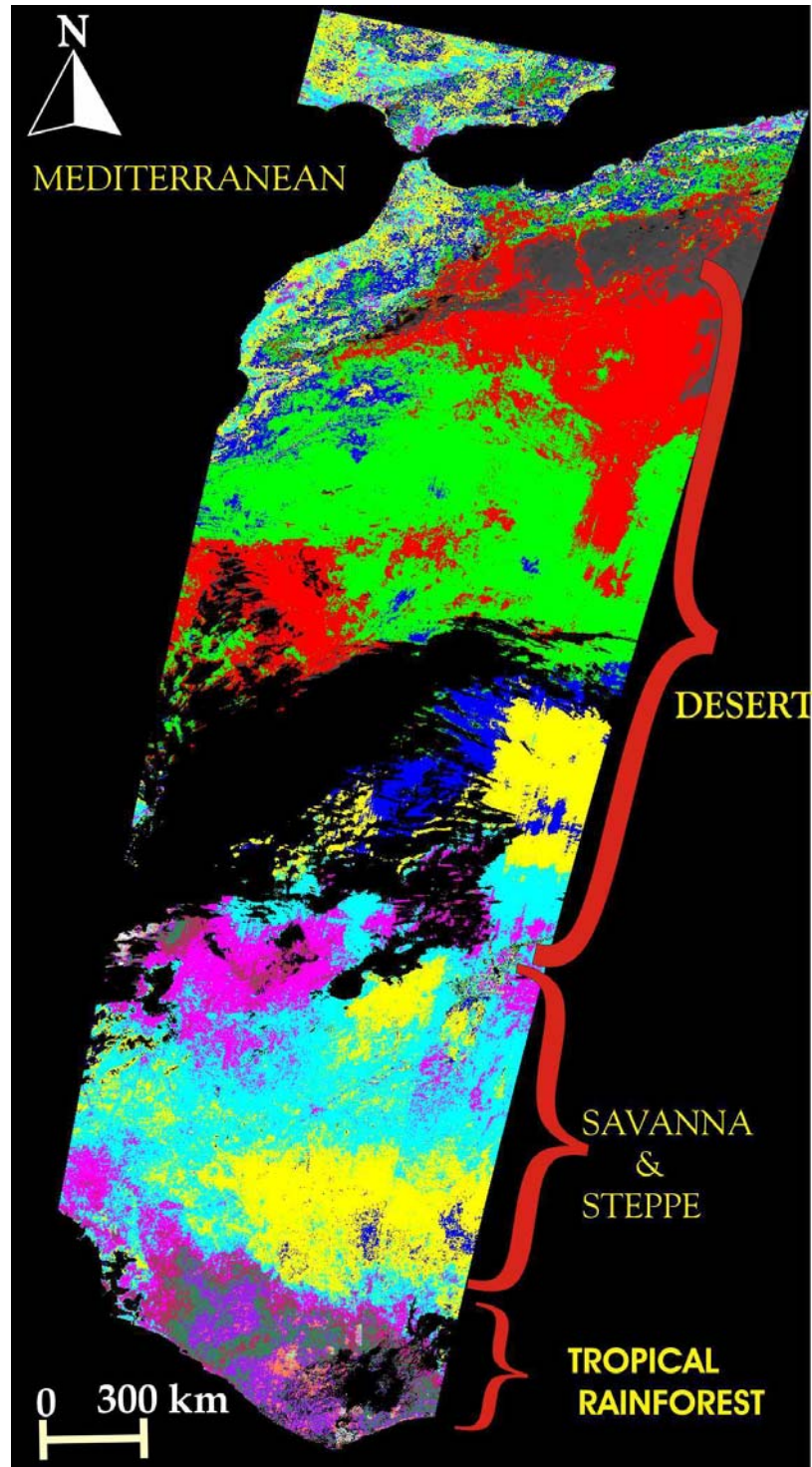


Figure 14 Vegetation types superimposed on an MTCI for West Africa.

### 3.1.3.2. Spatial resolution

MTCI variation with spatial resolution was evaluated by resampling full resolution MERIS data of the study area to various spatial resolutions. Eight different spatial resolutions, starting from 300 m to 2400 m with an increase of 300 m in each step, were considered in this experiment. Two different variables were estimated for these eight data sets i.e. Standard Deviation (SD) of MTCI in the whole scene (figure 15) and cumulative percentage of MTCI maximum (figure 13). It was observed that (i) as spatial resolution increased SD decreased. This trend was expected, as we were decreasing the variability by averaging neighbouring pixels. However this variation in the SD of MTCI was very low ( $<0.04$ ). (ii) the cumulative percentage of MTCI maximum for different spatial resolution has the same trend. On the basis of above two observations it can be concluded that spatial resolution has very little influence on MTCI values.

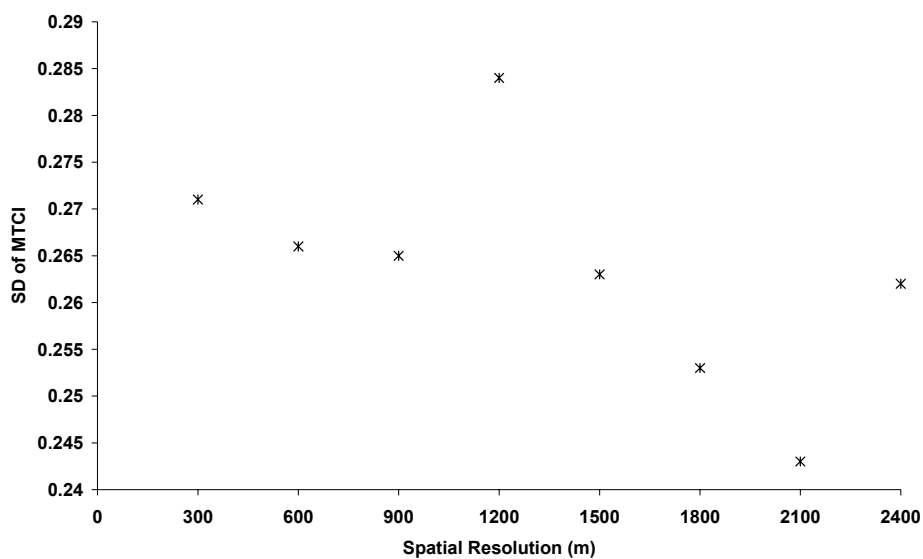


Figure 15. SD of MTCI for different spatial resolutions.

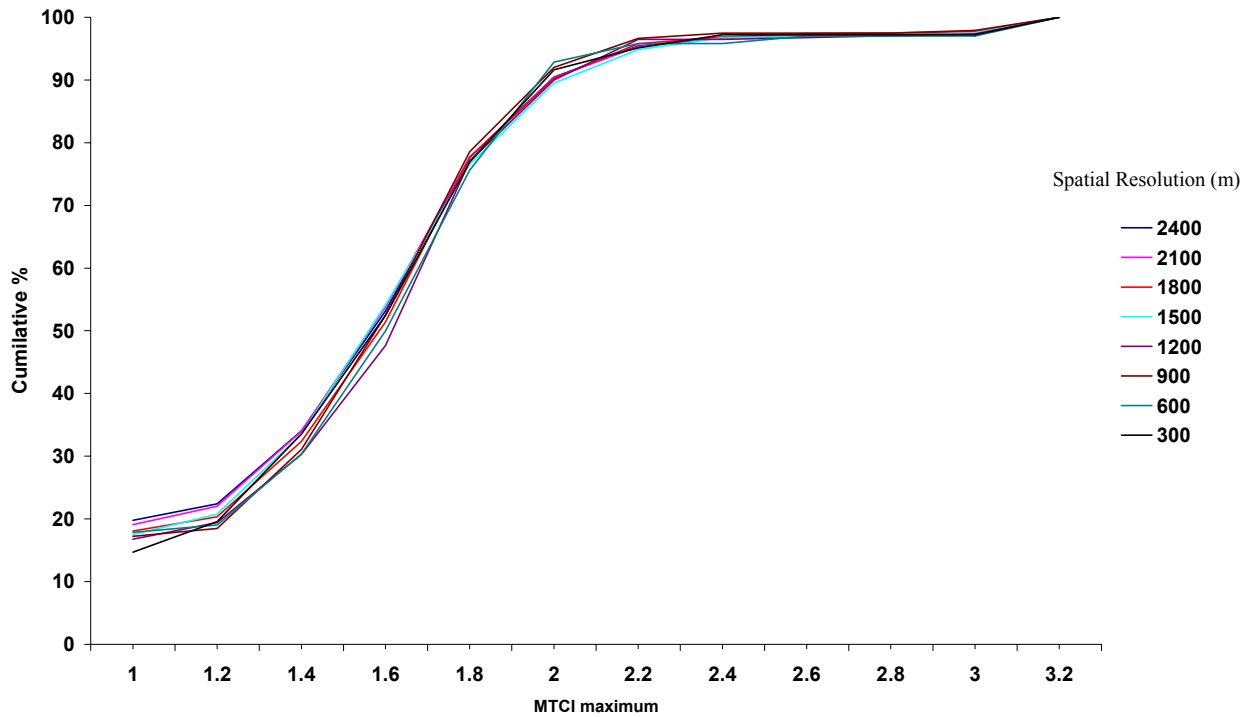


Figure 16. Cumulative percentage of MTCI maximum for different spatial resolutions.

### 3.1.3.3. Soil brightness

Effect of change in soil brightness (soil type 2, 3, 4, 5, 6 (Price, 1995)) on MTCI was evaluated by using an approach based on the signal-to-noise ratio (SNR) of data (Leprieur et al, 1994). It was found that MTCI is nearly insensitive to change in soil brightness.

### 3.1.3.4. View angle

The reflectance in bands 8, 9 and 10 changes differently with a change in the sensor viewing angle. Therefore, the MTCI values change with change in sensor viewing angle. Leprieur method was used to evaluate the sensitivity of MTCI for change in viewing angle. It was found that MTCI was sensitive to change in view angle, however, it was limited sensitive to change in viewing angle

between  $-30^\circ$  to  $+30^\circ$ . Therefore, care must be taken while estimating MTCI for different viewing angles.

## 3.2. Practical considerations

### 3.2.1 Calibration and validation

Direct MTCI evaluation was undertaken in a greenhouse for spinach (*Spinacia oleracea*) plants under controlled conditions. Reflectance spectra were measured using a GER 1500 spectroradiometer and chlorophyll was extracted and measured using specific absorption coefficients. The coefficients of determination ( $r^2$ ) between chlorophyll content and first MTCI and second REP were 0.65 and 0.6. This suggests a stronger MTCI-chlorophyll content relationship than REP-chlorophyll content relationship.

For all sample following were calculated:

1. Simple Ratio (SR) =  $\frac{R_{NIR}}{R_{Red}}$  (3)

Where  $R_{NIR}$  and  $R_{Red}$  are reflectances in NIR and red wavelengths respectively.

2. Normalised Difference Vegetation Index (NDVI) =  $\frac{R_{NIR} - R_{Red}}{R_{NIR} + R_{Red}}$  (4)

Where  $R_{NIR}$  and  $R_{Red}$  are reflectances in NIR and red wavelengths respectively.

3. REP estimated using the maximum of first derivative of the reflectance spectra. The derivative spectrum can be estimated by

$$D_{\lambda(i)} = \frac{R_{\lambda(i)} - R_{\lambda(i-1)}}{\Delta\lambda} \quad (5)$$

Where,  $R_{\lambda(i)}$  and  $R_{\lambda(i-1)}$  are reflectances at wavelength  $i$  and  $(i-1)$  respectively.

4. REP estimated using the linear interpolation (Guyot *et al.*, 1988).

$$REP = 700 + 40 \frac{(R_i - R_{700})}{(R_{740} - R_{700})} \quad (6)$$

$$\text{where } R_i = \frac{(R_{670} + R_{780})}{2}$$

Where  $R_{670}$ ,  $R_{700}$ ,  $R_{740}$  and  $R_{780}$  are reflectance at wavelength 670 nm, 700 nm, 740 nm and 780nm respectively.

5. REP estimated using Lagrangian interpolation (Dawson & Curran, 1998).

$$REP = \frac{A(\lambda_i + \lambda_{i+1}) + B(\lambda_{i-1} + \lambda_{i+1}) + C(\lambda_{i-1} + \lambda_i)}{2(A + B + C)} \quad (7)$$

$$\text{Where, } A = \frac{D\lambda_{(i-1)}}{(\lambda_{i-1} - \lambda_i)(\lambda_{i-1} - \lambda_{i+1})}, \quad B = \frac{D\lambda_{(i)}}{(\lambda_i - \lambda_{i-1})(\lambda_i - \lambda_{i+1})},$$

$$C = \frac{D\lambda_{(i+1)}}{(\lambda_{i+1} - \lambda_{i-1})(\lambda_{i+1} - \lambda_i)}$$

In this case  $D\lambda_{(i-1)}$ ,  $D\lambda_{(i)}$ ,  $D\lambda_{(i+1)}$  are the first derivative reflectances corresponding to wavebands  $\lambda_{(i-1)}$ ,  $\lambda_{(i)}$ ,  $\lambda_{(i+1)}$  respectively ( $\lambda_{(i)}$  is the band with maximum first derivative reflectance with  $\lambda_{(i-1)}$  and  $\lambda_{(i+1)}$  representing the bands either side of it).

6. Medium Resolution Imaging Spectrometer (MERIS) Terrestrial Chlorophyll Index (MTCI)  
(Dash & Curran, 2004)

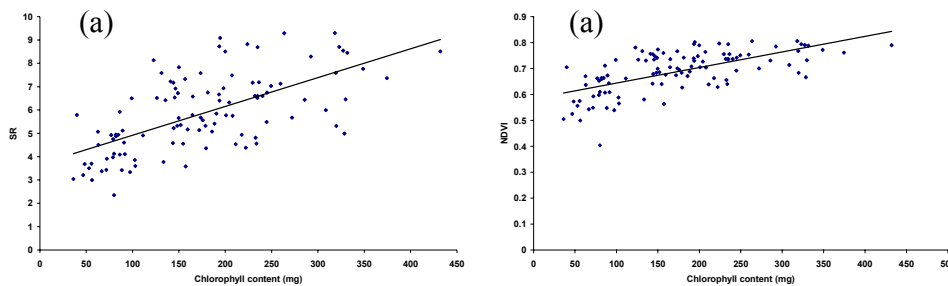
$$MTCI = \frac{R_{Band10} - R_{Band9}}{R_{Band9} - R_{Band8}} = \frac{R_{753.75} - R_{708.75}}{R_{708.75} - R_{681.25}} \quad (8)$$

Where  $R_{753.75}$ ,  $R_{708.75}$ ,  $R_{681.25}$  are the normalised surface reflectance in the centre wavelengths of band 8, 9 and 10 in the MERIS standard band setting

Reflectance indices	Chlorophyll content (mg)
<b>SR</b>	0.41
<b>NDVI</b>	0.4
<b>REP (Max first derivative)</b>	0.42
<b>REP (linear)</b>	0.55
<b>REP (Lagrangian)</b>	0.51
<b>MTCI</b>	0.58

Table 2. Correlation coefficient between the reflectance indices and chlorophyll content for spinach sample.

MTCI had the strongest ( $r^2 = 0.58$ ) and NDVI had the weakest ( $r^2 = 0.4$ ) positive correlation with chlorophyll content (table 2). Among the techniques used to estimate the REP, linear interpolation had the strongest ( $r^2 = 0.55$ ) and maximum of first derivative had the weakest ( $r^2 = 0.42$ ) correlation with chlorophyll content. Among all reflectance indices, the regression line for NDVI had the gentler slope, indicating less sensitivity to a change in chlorophyll content.



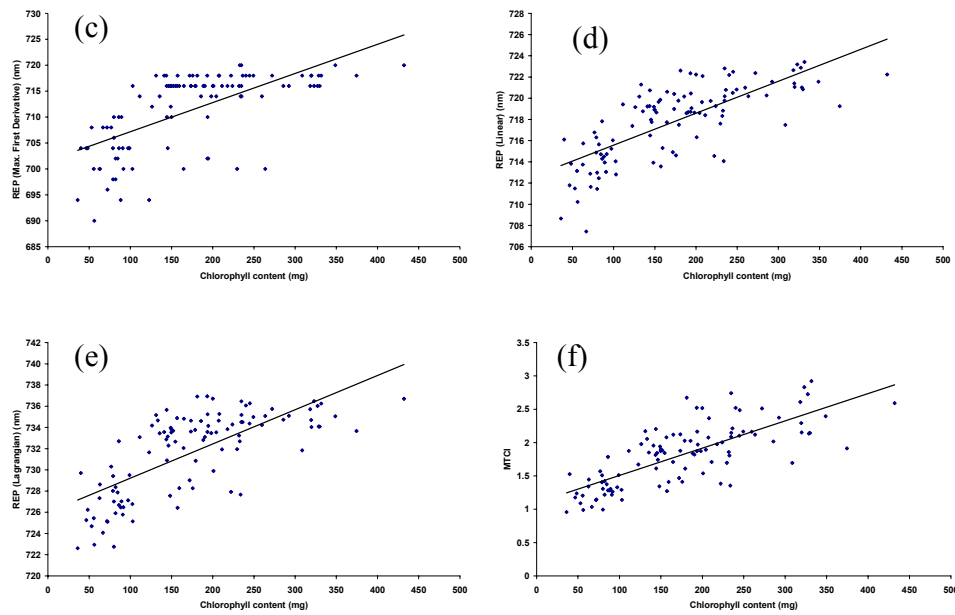


Figure 17. Relationship between chlorophyll content and SR (a), NDVI (b), REP estimated by maximum of first derivative (c), REP estimated by linear interpolation (d), REP estimated by Lagrangian interpolation (e) and MTCI (f) for spinach.

### 3.2.2 Quality control and diagnostics

Five 1-bit flags were generated to deal with different potential problems. The default values of all flags were 0, which represented nominal or acceptable conditions. The following conditions describe error or exception conditions, which were flagged by setting the corresponding bit to 1.

1. The land flag (LAND) was set to 1 if any pixel was not a land pixel.
2. The saturation flag (SATU) was set to 1 if any of the 3 spectral bands (band 8, 9 and 10) used by this algorithm were saturated.
3. The band flag (BAND) was set to 1 if data in one or more spectral bands was missing.
4. The overflow flag (OVER) was set to 1 if numerical overflow occurred while processing the data.

5. The underflow flag (UNDR) was set to 1 if numerical underflow occurred while processing the data.

Further possible improvement of this flag system is described in section 4.2.

### **3.2.3 Output**

The output generated by this algorithm was an index assigned as a real number. It was found MTCI value could reach 10 or more in some exceptional cases for example, MTCI was found to be more than 10 for sediment laden water. Based on the experiment described in section 3.1.3.1., the minimum and maximum range for MTCI was set to 0 and 4.2 respectively for scaling into 1 to 255 DN. The following three conditions were considered when producing the output.

1. If one of the four flags SATU, BAND, OVER or UNDR was set to 1, MTCI was not computed and its value was set to 1.
2. If all flags were set to 0 and if the value of MTCI was less than 0, then the value of MTCI was set to 1.
3. If all flags were set to 0 and if the value of MTCI was greater than 5.5, then the value of MTCI was set to 1.

If all quality flags were set to 0, the value of MTCI was computed and reported.

## **4. Assumptions and limitations**

### **4.1. Assumptions**

The following assumptions were made in the design of the MTCI algorithm.

1. All water pixels masked prior to estimation of MTCI.
2. Non-saturated MERIS level 2 normalised surface reflectances available in 681nm, 708 nm and 753nm spectral bands.

3. Positive Level 2 normalised surface reflectances in 681nm, 708 nm and 753nm spectral bands.
4. Level 2 normalised surface reflectances used as input corrected for the seasonally variable distance between the Earth and Sun.
5. MTCI values more than 5.5 set to 1.
6. Adjacency effects ignored.
7. Substantial atmospheric aerosol loads, as observed in dust storms and heavily polluted area screened out or their occurrence was infrequent.

## **4.2. Limitations**

The current version of the algorithm may have the following limitations.

1. Leaf Area Index: Chlorophyll content varies with the amount of chlorophyll in the vegetation and the amount of vegetation. Therefore, if chlorophyll concentration is constant then change in LAI will change reflectance. The effect of LAI on the MTCI estimation will be investigated.
2. Florescence: Leaf florescence has a maximum reflection at 690 nm in the red region. However florescence effects on canopy level reflectance is still unclear. The effect of florescence, on MTCI has not been considered.
3. Absorption due to other leaf components: Leaves contain several pigments, besides chlorophyll, that absorb radiation in red wavelengths; these could alter MTCI independently of chlorophyll concentration. However it was assumed that this effect is not significant at a regional scale using MERIS sensor. Effect of absorption due to other leaf components on MTCI estimation has not been considered.

## 5. References

- CLEVERS, J. G. P. W., DE JONG, S. M., EPEMA, G. F., VAN DER MEER, F., BAKKER, W. H., SKIDMORE, A. K. and SCHOLTE, K. H., 2002, Derivation of the red edge index using the MERIS standard band setting. *International Journal of Remote Sensing*, **23**, 3169-3184.
- CURRAN, P. J., 1989, Remote sensing of foliar chemistry. *Remote Sensing of Environment*, **30**, 271-278.
- CURRAN, P. J., DUNGAN, J. L. and GHOLZ, H. L., 1990, Exploring the relationship between reflectance red edge and chlorophyll content in slash pine. *Tree Physiology*, **7**, 33-48.
- CURRAN, P. J., KUPIEC, J. A. and SMITH, G. M., 1997, Remote sensing the biochemical composition of a slash pine canopy. *IEEE Transactions on Geoscience and Remote Sensing*, **35**, 415-420.
- CURRAN, P. J., 2001, Imaging spectrometry for ecological applications. *International Journal of Applied Earth Observation and Geoinformation*, **3**, 305-312.
- CURRAN, P. J. and STEELE, C. M., 2005, MERIS: The re-branding of an ocean sensor. *International Journal of Remote Sensing*, **26**, 1781-1798.
- DASH, J. and CURRAN, P. J., 2004, The MERIS Terrestrial Chlorophyll Index. *International Journal of Remote Sensing*, **25**, pp. 5003-5013.
- DAWSON, T. P., CURRAN, P. J. and PLUMMER, S. E., 1998, LIBERTY - Modelling the effects of leaf biochemical concentration on reflectance spectra. *Remote Sensing of Environment*, **65**, 50-60.
- DAWSON, T. P. and CURRAN, P. J., 1998, A new technique for interpolating the reflectance red edge position. *International Journal of Remote Sensing*, **19**, 2133-2139.

- DAWSON, T. P., 2000, The potential of estimating chlorophyll content from a vegetation canopy using the Medium Resolution Imaging Spectrometer (MERIS). *International Journal of Remote Sensing*, **21**, 2043-2051.
- FILELLA, I. and PEÑUELAS, J., 1994, The red edge position and shape as indicators of plant chlorophyll content, biomass and hydric status. *International Journal of Remote Sensing*, **15**, 1459-1470.
- GUYOT, G., BARET, F. and MAJOR, D. J., 1988, High spectral resolution: Determination of spectral shifts between the red and the near infrared. *International Archives of Photogrammetry and Remote Sensing*, **11**, 740-760.
- HORLER, D. N. H., DOCKRAY, M. and BARBER, J., 1983, The red edge of plant leaf reflectance. *International Journal of Remote Sensing*, **4**, 273-288.
- JAGO, R. A., CUTLER, M. E. and CURRAN, P. J., 1999, Estimation of canopy chlorophyll concentration from field and airborne spectra. *Remote Sensing of Environment*, **68**, 217-224.
- JEFFREY, A., 1985, *Mathematics for Engineers and Scientists*. (Workingham, UK: Van Nostrand Reinhold), pp. 708-709.
- JOHNSON, L. F., 1999, Response of grape leaf spectra to *Phylloxera* infestation. *NASA Report#CR-208765*, NASA Center for AeroSpace Information, Hanover, MD 21076-1320.
- LAMB, D. W., STEYN-ROSS, M., SCHAARE, P., HANNA, M. M., SILVESTER, W. and STEYN-ROSS, A., 2002, Estimating leaf nitrogen concentration in ryegrass (*Lolium* spp) pasture using chlorophyll red-edge: theoretical modelling and experimental observation. *International Journal of Remote Sensing*, **23**, 3619-3648.

- MUNDEN, R., CURRAN, P. J. and CATT, J. A., 1994, The relationship between red edge and chlorophyll concentration in the Broadbalk winter wheat experiment at Rothamsted. *International Journal of Remote Sensing*, **15**, 705-709.
- RAHMAN, H. and DEDIEU, G., 1994, SMAC: A simplified method for the atmospheric correction of satellite measurements in the solar spectrum. *International Journal of Remote Sensing*, **15**, 123-143.
- RAST, M., BÉZY, J.L., BRUZZI, S. The ESA medium resolution imaging spectrometer (MERIS): a review of the instruments and its mission, *International Journal of Remote Sensing*, **20**, 1681-1702, 1999.
- VERHOEF, W., 1984, Light scattering by leaf layers with application to canopy reflectance modelling: The SAIL model. *Remote Sensing of Environment*, **16**, 125-141.
- VERSTRAETE, M. M., PINTY, B. and CURRAN, P. J., 1999, MERIS potential for land application. *International Journal of Remote Sensing*, **20**, 1747-1756.
- YODER, B. and JOHNSON, L., 1999, *Seedling Canopy Chemistry, 1992-1993 (ACCP)* (Accelerated Canopy Chemistry Program). Data set. Available on-line [<http://www.daac.ornl.gov>] from Oak Ridge National Laboratory Distributed Active Archive Center, Oak Ridge, Tennessee, U.S.A.,

MTCI MAXIMUM	SITE#1		SITE#2		SITE#3		SITE#4		SITE#5		SITE#6		SITE#7		SITE#8	
	L2%	AC%	L2%	AC%	L2%	AC%	L2%	AC%	L25	AC%	L2%	AC%	L2%	AC%	L2%	AC%
1	4.1	.0	.0	.0	.5	.0	.0	.0	.0	.0	.0	.0	.2	.0	.0	.0
1.2	4.1	.0	.0	.0	.5	.0	.0	.0	.0	.0	.0	.0	.2	.0	.0	.0
1.4	4.1	.0	.0	.0	.6	.0	.0	.0	.0	.0	.0	.0	.3	.0	.0	.0
1.6	4.1	.0	.1	.0	.7	.0	.0	.0	.0	.0	.0	.0	.4	.0	.0	.0
1.8	4.1	.0	.3	.0	1.1	.0	.2	.0	.0	.0	.1	.2	.5	.0	.0	.0
2	4.1	.0	.9	.1	2.1	.1	.8	.0	.0	.0	1.3	1.8	.6	.0	.0	.0
2.2	4.2	.0	2.9	.6	6.4	1.9	2.3	.4	.8	1.3	5.2	4.3	1.3	.0	.0	.0
2.4	5.1	.0	7.0	1.2	26.0	13.5	23.3	11.3	9.3	19.8	14.2	9.6	3.7	2.5%	.5	3.4
2.6	7.9	.0	24.5	3.5	76.3	63.7	86.7	74.7	45.5	62.9	32.0	27.8	17.0	32.1	9.3	22.5
2.8	35.1	18.2	90.1	30.6	97.6	95.2	98.5	97.9	84.3	94.5	60.6	67.4	65.1	77.5	44.0	58.2
3	79.6	78.9	99.3	92.9	99.8	99.8	100.0	100.0	99.2	100.0	89.5	95.2	97.6	99.2	82.3	90.9
3.2	96.3	95.3	99.9	99.9	99.9	100.0	100.0	100.0	100.0	100.0	98.2	99.8	100.0	100.0	97.9	99.4
3.4	98.0	100.0	99.9	100.0	100.0	100.0	100.0	100.0	100.0	100.0	99.6	100.0	100.0	100.0	99.9	99.9
3.6	98.4	100.0	99.9	100.0	100.0	100.0	100.0	100.0	100.0	100.0	99.8	100.0	100.0	100.0	100.0	100.0
3.8	98.5	100.0	100.0	100.0	100.0	100.0	100.0	100.0	100.0	100.0	100.0	100.0	100.0	100.0	100.0	100.0
4	98.5	100.0	100.0	100.0	100.0	100.0	100.0	100.0	100.0	100.0	100.0	100.0	100.0	100.0	100.0	100.0

Table 3. Comparison of cumulative % of MTCI ranges for MTCI estimated from L2 data (L2) and atmospherically corrected L1 data (AC) for Vietnam

MTCI MAXIMUM	SITE#1		SITE#2		SITE#3	
	L2%	AC%	L2%	AC%	L2%	AC%
1	.0	.0	.0	.0	.0	.0
1.2	.0	.0	.0	.0	.0	.0
1.4	.3	1.6	.0	.0	.2	.0
1.6	5.6	9.9	.0	.7	1.1	.2
1.8	13.5	17.1	.7	2.1	7.4	.5
2	24.7	29.9	2.5	3.9	22.9	4.0
2.2	42.1	48.0	4.3	10.1	41.7	15.8
2.4	58.9	65.8	10.0	19.0	64.2	34.8
2.6	74.3	79.9	19.2	32.3	79.3	54.3
2.8	85.2	92.1	32.4	49.3	88.9	73.1
3	95.7	97.7	47.8	62.5	94.6	84.8
3.2	99.0	99.3	61.2	75.9	97.1	91.5
3.4	100.0	100.0	74.0	87.3	98.9	96.0
3.6	100.0	100.0	85.9	94.9	99.8	98.2
3.8	100.0	100.0	93.6	98.2	99.8	99.1
4	100.0	100.0	97.5	99.6	99.8	100.0
4.2	100.0	100.0	99.3	100.0	100.0	100.0
4.4	100.0	100.0	100.0	100.0	100.0	100.0

Table 4 Comparison of cumulative percentage of MTCI ranges for MTCI estimated from L2 data (L2) and atmospherically corrected L1 data (AC) for UK

MTCI MAXIMUM	Deciduous forest		Mediterranean		Savanna1		Savanna2		Tropical rain forest	
	L2%	AC%	L2%	AC%	L2%	AC%	L2%	AC%	L2%	AC%
1	.0	.0	.2	6.3	.0	.0	.0	.7	.0	.0
1.2	.0	.0	.3	30.5	1.3	7.5	9.2	77.5	.0	.0
1.4	.0	.1	.5	65.3	64.6	74.1	95.5	99.8	.0	.0
1.6	.0	.6	5.7	86.4	97.7	98.4	100.0	100.0	.0	.0
1.8	.2	2.5	34.3	97.4	99.5	99.8	100.0	100.0	.0	.0
2	2.2	9.6	69.2	99.4	100.0	100.0	100.0	100.0	.0	.0
2.2	10.1	33.9	88.3	99.9	100.0	100.0	100.0	100.0	.0	.0
2.4	35.0	62.9	97.4	99.9	100.0	100.0	100.0	100.0	.1	.6
2.6	66.6	80.0	99.5	99.9	100.0	100.0	100.0	100.0	2.7	5.8
2.8	83.5	92.4	99.9	99.9	100.0	100.0	100.0	100.0	8.2	30.1
3	93.7	99.1	100.0	99.9	100.0	100.0	100.0	100.0	25.3	74.5
3.2	98.6	100.0	100.0	99.9	100.0	100.0	100.0	100.0	72.6	97.9
3.4	100.0	100.0	100.0	99.9	100.0	100.0	100.0	100.0	96.8	99.9
3.6	100.0	100.0	100.0	99.9	100.0	100.0	100.0	100.0	99.8	100.0
3.8	100.0	100.0	100.0	100.0	100.0	100.0	100.0	100.0	100.0	100.0
4	100.0	100.0	100.0	100.0	100.0	100.0	100.0	100.0	100.0	100.0

Table 5 Comparison of cumulative percentage of MTCI ranges for MTCI estimated directly from L2 data (L2) and atmospherically corrected L1 data (AC) for West Africa.